

國立交通大學

機械工程學系

博士論文

多自由度電熱式微致動器的研究

The Developments of Electro-Thermal Driven
Microactuators with Multi-Dimensional Motions

研究生：吳青臺

指導老師：徐文祥 教授

中華民國九十四年六月

多自由度電熱式

微致動器的研究

**The Developments of Electro-Thermal Driven
Microactuators with Multi-Dimensional Motions**

研究生：吳青臺

Student : Chientai Wu

指導教授：徐文祥

Advisor : Wensyang Hsu

國立交通大學

機械工程學系

博士論文

A Dissertation

Submitted to Department of Mechanical Engineering

College of Engineering

National Chiao Tung University

in partial Fulfillment of the Requirements

for the Degree of

Ph.D

in

Mechanical Engineering

June 2005

Hsinchu, Taiwan, Republic of China

中華民國九十四年六月

多自由度電熱式微致動器的研究

學生：吳青臺

指導老師：徐文祥 教授

國立交通大學機械工程學系

摘 要

在以往的文獻中，大部分的微致動器僅能在一個自由度內運動，本論文的研究目的在於設計及製造出兩種多自由度電熱式微致動器。一種是除了能於垂直方向運動外，更特別的是這種微致動器還能於立體空間中做水平方向的致動；第二種致動器則是一種可做為多階微傳送器單元的電熱式微致動器。

第一種電熱式微致動器，能於垂直方向運動，是因為這種微致動器具有一垂直可調單元(高度調整器)，由於上下層不同材料間的殘留應力差及受熱時的雙層板效應，使得垂直可調單元(高度調整器)可產生垂直方向的調整和運動，以此垂直可調單元(高度調整器)為基礎，再加上兩支不同截面積但相同長度的鄰接樑，兩支鄰接樑被加熱時由於不對稱的熱膨脹關係因此會產生側向位移，形成了側向運動單元，整合垂直可調單元(高度調整器)及側向運動單元完成了本論文的具兩度空間運動特性的電熱式微致動器。

第二種電熱式微致動器，則是在垂直可調單元(高度調整器)的末端，橫向方向加上了兩個雙層板結構，由於雙層板間的殘留應力差，當犧牲層被去掉後，這兩個雙層板結構就會自動彎曲向上，形成兩支傳送臂且避免了沾黏現象的發生，輔以垂直可調單元(高度調整器)與兩支傳送臂，各自獨立的電路設計，整體構成了一種可依被傳送物重量而改變傳送高度的多階微傳送器單元。

這裏所提出的兩種微致動器都可以面加工的方式做批次化的製造，第一種電熱式微致動器是由 MUMPS 的製作方式所完成的，特別的是本論文發展了兩階段去除犧牲層的方法，使得在最後去除犧牲層時不致同時去掉犧牲層和連接側向運動單元的連接層；第二種電熱式微致動器則是利用兩種高分子聚合物的高熱膨脹係數差及絕緣的特性，來當作主結構材料並簡化了製程。

經由測試，第一種電熱式微致動器，在輸入電壓為 5 伏特的狀況下，可產生 10 μm 的側向位移，在相同大小輸入電壓下，垂直可調單元(高度調整器)可產生 12 μm 的垂直位移；第二種電熱式微致動器，垂直可調單元(高度調整器)，在輸入電壓為 1 伏特的狀況下，可產生 5 μm 的垂直位移，而傳送臂則可在輸入電壓為 2 伏特的狀況下，產生 18 μm 的垂直位移；這兩種微致動器在不同的運動方向，由測試結果皆顯現了相當小的耦合效應；而有限元素分析軟體 ANSYS 5.7 的分析結果亦和本論文所做的測試相當吻合。



The Developments of Electro-Thermal Driven Microactuators with Multi-Dimensional Motions


Student: Chientai Wu

Advisor: Prof. Wensyang Hsu

Department of Mechanical Engineering

National Chiao-Tung University

ABSTRACT



In previous literatures, most of the microactuators were designed to deflect in one dimension only. The goal of this dissertation is to design and fabricate two kinds of electro-thermally driven microactuators with multi-dimensional motions. The first kind of electrothermal microactuator can deflect not only in vertical direction but also a lateral motion in space can be generated. The second one is featured with adjustable height that may act as a basic unit for multi-level conveyors.

The first kind of electrothermal microactuator has a vertical adjust unit (height adjuster). The vertical-adjustable unit (height adjuster) proposed here utilizes the bimorph effect and residual stresses of materials between the upper layer and the lower layer when they are heated. Two adjacent beams with different cross sections but the same length are connected with the basis of

vertical-adjustable unit (height adjuster). These two beams produce asymmetrical thermal expansions, which lead to lateral deflection. Hence two-dimensional motions are obtained by combining the vertical and lateral deflections.

The second kind of electrothermal microactuator may act as a basic unit for multi-level conveyors. This microactuator is based on principle of thermal bimorph actuation with two long conveying fingers to exert out-of-plane bending motions in the transversal direction. The fingers are connected and lifted by an initially curved height adjuster in the longitudinal direction. The devices can provide conveyance of micro-objects between two plane levels of different heights.

The microactuators proposed here are both fabricated by surface micromaching technique. The first kind of electrothermal microactuator is fabricated by MUMPs process. Especially a two-step releasing method is used here to free the microactuator successfully. This method makes the sacrificial layer and the connection layer for lateral driven unit be etched step-by-step in final releasing process. For the second kind of electrothermal microactuator, two types of polymer materials are used to the main structure, owing to their large difference on thermal expansion coefficient and electrical insulation characterization.

The testing results show that the first kind of electrothermal microactuator with its lateral driven unit($600\ \mu\text{m} \times 24\ \mu\text{m} \times 2\ \mu\text{m}$) can produce $10\ \mu\text{m}$ lateral

displacements at input voltages of 5 volts. The vertical-adjustable unit (height adjuster) with dimension of $70\ \mu\text{m} \times 10\ \mu\text{m} \times 2.5\ \mu\text{m}$ at 5 volts can produce about $12\ \mu\text{m}$ downward displacement. The second microactuator with overall dimension of $900\ \mu\text{m} \times 100\ \mu\text{m} \times 4.5\ \mu\text{m}$ can provide $5\ \mu\text{m}$ vertical displacements by vertical-adjustable unit (height adjuster) at 1 volt and $18\ \mu\text{m}$ lateral displacements by conveying finger at 2 volts. Both proposed microactuators can exhibit controllable motions in different directions independently. Simulations conducted by finite-element program ANSYS 5.7 show the results widely match with testing results.



誌 謝

由衷感謝徐文祥老師對我辛勤的教導。徐老師對我不僅只是在課業上的指導，在我的工作及為人處事上，徐老師亦總能適時的幫我釐清事情的輕重緩急並給予我適切的思考方向，特別是畢業前我仍為工作上的壓力所苦，老師的臨門一腳，讓我從泥濘裡站起來，否則至今我將仍在博士學位門外徘徊。

很榮幸的，能邀請到學術研究成果豐碩的學者教授，成為末學的口試委員，深深感謝陳榮順教授、陳仁浩教授、范士岡教授、羅一中教授，對學生的論文研究，提出許多值得深思探討的建議，給予末學更多元的研究方向。

交通大學奈微米機電實驗室，是一個最溫馨及最合諧的實驗室。感謝鎮鵬、政璋、正軒在博士班的這幾年，常常一同討論，激發創意，特別是鎮鵬，更要感謝你的鼎力協助。實驗室優秀的學妹、學弟們，君煒、涵評、金傳、文川、守仁、秀玲、春蘭就像我的守護天使般，陪我一同走過。感謝交大半導體中心的葉雙得先生、徐秀巒、林素珠、范秀蘭與陳悅婷小姐，不知多少次麻煩了你們，非常感謝你們。

另外特別感謝廠長林長寶上校，在我最艱困的時候給我的支持與包容，讓我有機會完成學位並繼續報效國家，這份恩情我將永銘於心。第二零四廠規劃資訊全體同仁，炯堯、孟樵、冏暉、惠真....謝謝你們的相挺，讓我的軍旅生涯更加精采。

祖父母對我自幼的教育和養育是我永遠也不敢須臾或忘的，就讓這張博士畢業證書，長埋於您們的墓前，謝謝您們對孫兒這份無私無我的教養恩情。不擅表達、默默付出是母親的寫照，感謝您對我的照顧與擔憂；秋蘭、青霖、青藩、秋月、憶慧，謝謝你們對大哥的支持，也不要忘記我們兄弟姐妹的成長歷程。太太珍玉，妳一直是我精神最大的支柱，和妳結婚，讓我的生命有了改變，豐富且更有深度，感謝妳，辛苦了。僅以兒子存恩的名字，「心存感恩」的感謝這一路走來的一切一切。



CONTENTS

ABSTRACT (in Chinese)	i
ABSTRACT (in English)	iii
LIST OF TABLES	x
LIST OF FIGURES	xi
Chapter 1 INTRODUCTION	1
1.1. Background.....	1
1.2. Motivation	14
1.3. Dissertation Outline.....	16
Chapter 2 DESIGN AND SIMULATION	17
2.1. Concept Design	17
2.2. Simulation	20
Chapter 3 FABRICATION	24
3.1. Fabrication of an Electro-Thermally Driven Microactuator with Two Dimensional Motions.....	24
3.2. Fabrication of an Electro-Thermally Microactuator for Multi-Level Conveying	31
Chapter 4 CHARACTERIZATION AND RESULTS	34
4.1. Characterization of an Electro-Thermally Driven Microactuator with Two Dimensional Motions	34
4.2. Characterization of an Electro-Thermally Microactuator for Multi-Level Conveying	37
Chapter 5 CONCLUSIONS	42
5.1. Summary.....	42

5.2. Discussions.....43

REFERENCES..... 44



LIST OF TABLES

TABLE 1 THE TYPICAL ACTUATION PRINCIPLES IN MEMS.....9

TABLE 2 MATERIAL PROPERTIES USED IN SIMULATIONS..... 21



LIST OF FIGURES

FIGURE 1-1. SCHEMATIC DIAGRAM OF RESONANT COMB-DRIVE. [18].....	11
FIGURE 1-2. IN-PLANE MOTION OF MICROMOTOR. [19].....	11
FIGURE 1-3. OUT OF PLANE MOTION OF THE POLYIMIDE V-GROOVE JOINT. [21].....	12
FIGURE 1-4. THERMALLY DRIVEN CANTILEVER ACTUATOR MADE OF POLYIMIDE. [15].....	12
FIGURE 1-5. A C-SHAPE MICROACTUATOR. [22].....	13
FIGURE 2-1. SCHEMATIC VIEW OF THE PROPOSED ELECTRO-THERMALLY DRIVEN MICROACTUATOR.....	18
FIGURE 2-2. SCHEMATIC DRAWING OF THE PROPOSED MICROACTUATOR.....	19
FIGURE 2-3. OPERATION PRINCIPLE OF THE PROPOSED MULTI-LEVEL CONVEYOR.....	20
FIGURE 2-4. THE HEATER CIRCUIT LAYOUT OF THE DEVICE.....	20
FIGURE 2-5. THE HALF-SYMMETRICAL FINITE ELEMENT 3-D MODEL OF THE PROPOSED MICROACTUATOR.....	22
FIGURE 2-6. THE SIMULATED DOWNWARD DISPLACEMENTS OF THE FINGER UNDER DIFFERENT INPUT VOLTAGES.....	23
FIGURE 2-7. THE SIMULATED DOWNWARD DISPLACEMENTS OF THE HEIGHT ADJUSTER UNDER DIFFERENT INPUT VOLTAGES.....	23
FIGURE 3-1. FABRICATION PROCESS.....	25
FIGURE 3-2. THE INITIAL FABRICATION RESULT BY ONE-STEP RELEASING PROCESS.....	27
FIGURE 3-3. THE MOVING PLATE AND THE SUBSTRATE ARE STICTED TOGRTHER.....	28
FIGURE 3-4. THE FINAL FABRICATION RESULT BY MODIFIED TWO-STEP RELEASING PROCESS.	28
FIGURE 3-5. THE SEM OF THE HEIGHT ADJUSTER WITH MOVING PLATE.....	29
FIGURE 3-6. THE TOP VIEW OF THE FABRICATED RESULT OF THE MICROACTUATOR.....	29
FIGURE 3-7. THE SEM OF THE LATERAL DRIVEN UNIT.....	30
FIGURE 3-8. THE SEM OF THE HEIGHT ADJUSTER, MOVING PLATE AND CONTACTED PADS.	30
FIGURE 3-9. FABRICATION PROCESS.....	32
FIGURE 3-10. SCANNING ELECTRON MICROSCOPES OF THE FABRICATION RESULTS.....	33

FIGURE 3-11. CLOSE-UP VIEW OF THE FINGER.....	33
FIGURE 4-1. SCHEMATIC DRAWING OF THE MEASUREMENT SYSTEM.....	34
FIGURE 4-2. THE MEASURED LATERAL DISPLACEMENTS OF THE LATERAL DRIVEN UNIT UNDER DIFFERENT INPUT VOLTAGES.....	36
FIGURE 4-3. THE MEASURED DOWNWARD DISPLACEMENTS AT THE END OF THE MOVING PLATE UNDER DIFFERENT INPUT VOLTAGES.....	36
FIGURE 4-4. THE MEASURED DISPLACEMENTS IN COUPLING TEST WHERE THE LATERAL DRIVEN UNIT AND BIMORPH BEAMS ARE OPERATED AT THE SAME INPUT VOLTAGES SIMULTANEOUSLY.....	37
FIGURE 4-5. THE SIMULATED AND CALIBRATED DOWNWARD DISPLACEMENTS OF THE CONVEYING FINGER UNDER DIFFERENT INPUT DC VOLTAGES.....	40
FIGURE 4-6. THE SIMULATED AND CALIBRATED DOWNWARD DISPLACEMENT OF THE HEIGHT ADJUSTER UNDER DIFFERENT INPUT DC VOLTAGES.....	40
FIGURE 4-7. THE MEASURED DISPLACEMENTS AT THE END OF HEIGHT ADJUSTER IN COUPLING TEST, WHERE THE HEIGHT ADJUSTER IS ACTUATED FIRSTLY, AND THEN DIFFERENT INPUT VOLTAGES ARE APPLIED TO THE CONVEYING FINGERS.....	41
FIGURE 4-8. THE MEASURED DISPLACEMENTS OF FINGER TIP IN COUPLING TEST, WHERE THE FINGER IS ACTUATED FIRST, AND THEN DIFFERENT INPUT VOLTAGES ARE APPLIED ON THE HEIGHT ADJUSTER.....	41

Chapter 1

INTRODUCTION

1.1. Background

Microelectromechanical system(MEMS) is a device that consists of micromachine and microelectronic, where the micromachines are controlled by microelectronics. It is often fabricated using micromaching technology and an integrated-circuit(IC) process. Therefore, the MEMS have the characteristics of miniature(size in μm degree), multiplicity (IC processing) and microelectronic, which will play a decisive role in the development of future technology.

The silicon-based micromachining is a fundamental tool for MEMS fabrication that can be divided into bulk-micromachining and surface-micromachining. Bulk silicon micromachining, used to selectively remove significant amounts of silicon from substrates by wet, vapor-phase, or plasma-phase etching, provides structures such as membranes, grooves, cavities, and undercutting of delicate or high-aspect-ratio microstructures. The features in bulk micromachining are sculpted in materials, such as single crystal silicon, quartz, SiC, GaAs, InP, and Ge, by orientation-independent called isotropic or orientation-dependent called anisotropic etching. Surface micromachining is characterized by deposited “thin” films commonly used in IC fabrication such as polysilicon, silicon oxide, silicon nitrides, and metals to fabricate the MEMS

structures. The features of that are built up, layer by layer, on the surface of a substrate, for example a single crystal silicon wafer (SC silicon). Either dry or wet etching, in chemical reaction, could be defined the features of the structures in the upper-plane of substrate and also be released them from the plane by undercutting. Furthermore, the main structures could be suspended after the thick layer under that is applied as sacrificial layer and is released by wet or dry etching.

Non-silicon based micromachining is another important tool for MEMS, which can be categorized by whether fabrication process involves lithography or not. The LIGA and SLIGA (Surface micromachining and LIGA) utilize thick photoresist technique, deep X-ray lithography, and electroplating to implement high resolution, precise and high-aspect-ratio metal micromechanical structures. Owing to the high cost of using synchrotron radiation, UV-LIGA is developed by using low-cost ultraviolet light source with lower resolution and contrast as trade-off. The other non-silicon based methods are precise manufacturing tools such as EDM (electro-discharge machining), excimer laser machining, ion beam machining, cutting, milling, forging, moulding, and embossing used to construct three-dimensional MEMS structures or for special purposes.

Generally, MEMS can be defined as the functional integrations of mechanical, chemical, fluid-dynamic, biological, electrical, electronic, optical, and other functional components [1].

Using micromachining technology may have many advantages, which includes high throughput, high accuracy, gentleness and performance improved

[2]. When the scale of the devices is reduced into micro scale, then some physical quantities become very important than they are in the macro scale. For example in magnetic forces, the current density of a micro coil can be much higher than in a large coil. Therefore, the higher force due to current density increasing by a factor of ten is owing to the size decreases by a factor of ten [3]. Batch of fabrication processes is another strong point using MEMS technology. These processes can allow the production of many identical components at the same time on one chip, therefore the lower processing cost for each individual device can be achieved than the conventional machining.

Research and development in MEMS have made remarkable progress since 1988, when an electrostatic micromotor in size of a human hair was first operated successfully by Fan, Tai, and Muller [4]. Since then, many types of microactuators utilizing various driving forces and mechanisms have been developed. The prospective applications of microactuators can be divided into several categories, including optics, communication and information apparatus, transportation and aerospace, robotics, fluidics and chemical analysis systems, biotechnologies, medical engineering, and microscopy [5-7]. However, present microactuators are still primitive and most of them cannot transmit large forces and motions to external world.

MEMS technology is essentially an application driven technology. The evolution and maturity of MEMS in the coming future will be driven not only by improvement on microfabrication technologies but by innovative, aggressive electromechanical systems design especially the microactuator technology.

Lots of MEMS commercial products come from the progress in microactuators by new design concepts and/or advanced fabrication technologies. Consequently, development of microactuators, which can satisfy specific requirements or can exhibit special functions, will accelerate MEMS applying in our daily life.

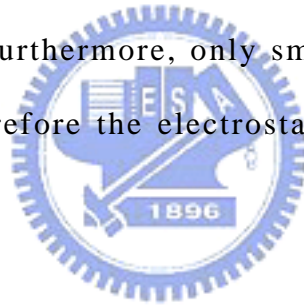
Usually, four major actuation principles, electrostatic, piezoelectric, electromagnetic, and thermal are used to driving the most of microactuators. Other driving sources of fluid, light, and chemical are also have been reported. Each principle has its own advantages and disadvantages. The choice of these approaches should match the requirements for particular applications. Following, the four major driving principles are described.

Electrostatic Actuation

The microactuators driven by electrostatic force is used coulomb force to exert the functions. The representative applications for the electrostatic microactuators are the micromotor [8-9], the comb drive microactuator [10], the scratch drive actuator (SDA) [11], and the vertical comb drive actuator [12]. The vertical driving mode uses a pair of parallel conductive plates with electrical potentials across two plates to form a parallel capacitor. The attractive forces between electrodes will keep bending the free electrode until mechanically balanced. The vertical driving mode exhibits nonlinear relation of force and displacement. Besides, the displacement is limited by the gap between electrodes. To generate large enough force at reasonable applied

voltage, the gap is generally smaller than 5 μm . On the contrary, lateral electrostatic actuation becomes important in linear motions with comb-like structures where the movable electrodes move in parallel to the fixed electrodes. The force-displacement relations are depending on the structure thickness, separation gap, and number of fingers. An efficient comb drive microactuator can be achieved by designing many thick comb fingers with narrow gap.

In general, electrostatic microactuators are compatible with CMOS processes and materials, little temperature dependent, little power, and benefits in scaling law. The electrostatic microactuators are sensitive to dust and humidity. Hence, to effectively actuate the devices, operation environments are restricted in vacuum. Furthermore, only small deflections can be achieved except in resonant state, therefore the electrostatic force may be restrictive for some applications.



Piezoelectric Actuation

The microactuators driven by piezoelectric force [13] are use the piezoelectricity property in certain materials such as PZT (lead zirconate titanate), ZnO, PVDF (polyvinylidene fluoride), and quartz to convert electrical energy into mechanical energy. The piezoelectrics produces charge on their surfaces when they are mechanically strained, or, conversely, they become strained upon application of an electric field. The force of piezoelectric actuator is quite large, the response time is very short, and efficiency is high if

the leakage current and hysteresis effect are kept under control. However, the fractional stroke (displacement per unit length) is quite small for monolayer structure, typically being no more than 0.2%. Therefore, to overcome these problems, thick or stacked structures and bimorph structures are used in macroscopic devices to obtain larger extension and bending motion respectively, but it is still difficult to fabricate this type of element in the micro domain. Further, in application, direction dependent and temperature dependent piezoelectric coefficients of the piezoelectric materials must be taken into consideration. Beside the temperature during these processes is high, they are not easy compatible with CMOS processes except by sputtering. Comparing to electrostatic actuation, piezoelectric microactuators without the need of gaps can provide much greater forces with very quick response up to mega hertz. However, problems in reliable material deposition and microfabrication process still not matured.



Magnetic Actuation

The magnetic driven is usually based on the electromagnetic force [14]. The electromagnetic force is exerted on the coil (N-turns carrying current) in the magnetic field. However, joule heating of the coil will produce thermal problems and the current carrying capacity of the conductor need to be improved. Generally, magnetic microactuators exhibit advantages of large force, large stroke, high speed (around 1~100 kHz), low input voltage, and low wear in

operation. In addition, comparing to electrostatic actuation, magnetic actuation does not suffer catastrophic field breakdown. However, the volume of the integrated magnets limits and complicates miniaturization of these types of microactuators. Actuation is controlled by current switching rather than preferred voltage. A large force means a high current, leading to problems of power consumption and dissipation.

Thermal Actuation

Thermal microactuators usually can be categorized into two kinds, one is based on thermal expansion and the other is based on phase transformation such as shape memory alloy (SMA). Heat can be generated by different means including joule heating, light, chemical reaction, and employing junctions between dissimilar regions with temperature difference. Joule heating is the most popular among these heating methods. Generally, thermal microactuators exert large displacements and significant amount of forces at low driving voltages. Comparing to electrostatic and piezoelectric actuations, they are more power consumptive and slow response. However, thermal microactuators show good compatibility and simple integration with IC process [15].

For microactuators using gas/liquid state thermal expansions, they can exert tremendous force through a long stroke. However, these microactuators usually need a cavity or chamber to trap the gas or liquid that means a larger device space required. In addition, they usually dissipate more power and

response slowly than other types of thermal microactuators. The most popular type thermal microactuators are based on thermal expansion in solid state. Actuation mechanisms of these microactuators are mainly based on asymmetrical thermal expansions such as bimorph microactuators [16-17], hot-cold beam microactuators [18], and long-short beam actuator [19]. Another thermo-mechanical actuation is using SMA [20-21]. The shape memory effect occurs in certain alloy materials such as TiNi. They exhibit thermoelastic martensitic transformation leading to interesting shape recovery characteristics upon heating. The shape recovery occurs at a transformation temperature called austenite temperature (T_a). The austenite phase changes to the martensite phase upon cooling the alloy below a composition dependent transition temperature. This phase changes cause discontinuous volume changes of the material that can be much greater than simple thermal expansion of the solid. Therefore, SMA can produce very large force and displacement. However, its response is very slow and low efficiency. In addition, microfabrication of SMA is not matured and compatibility with IC process is still a problem.

To sum up, each actuation principle as shown in Table 1 has its own advantages and disadvantages. The choice and the optimization should be made according to the requirements of applications and the facilities available for fabrication.

Table 1. The typical actuation principles in MEMS

		Electrostatic	Piezoelectric	Magnetic	Thermal
Actuation Method		Attractive Force	Strain	Attractive Force Repulsive Force	Solid Expansion
Materials		Metal, Silicon, Polymer	Piezoelectrics: PZT, ZnO PVDF, Quartz	Ferromagnetic materials: NiFe	Large CTE Large difference of CTEs SMA: TiNi
Miniaturization		Easy	Difficult	Difficult	Easy
Input	Voltage	High	High	Low	Low
	Current	*	*	High	May High
	Power	Low	Low	High	Medium
Output	Displacement	Small	Small Large (Bending)	Large	Large
	Force	Small	Large	Large	Medium to Large
	Response	Fast	Very Fast	Fast	Slow
Operating Environment		Vacuum	Normal	Normal	Normal

Motion Directions

According to the motion directions of the microactuators, usually it can be categorized into in-plane and out-of-plane motion directions (included lateral and rotary motion) . Comb-drive as shown in Figure 1-1 [22], and micromotor as shown in Figure 1-2 [23] are the examples of in-plane motion. Deformable mirror [24], polyimide V-groove joint (Figure 1-3 [25]), cantilever actuator (Figure 1-4 [15]) and C-Shape actuator (Figure 1-5 [26]) are the examples of out-of-plane-motion. Despite the large number of papers on microactuators, very few have discussed the design and fabrication of microactuators to move more than one direction.



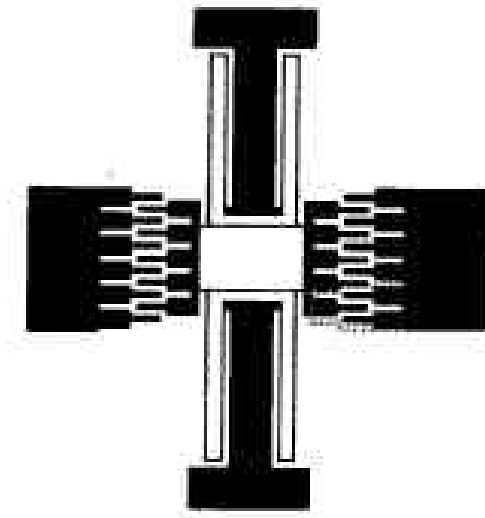


Figure 1-1. Schematic diagram of resonant comb-drive. [22]

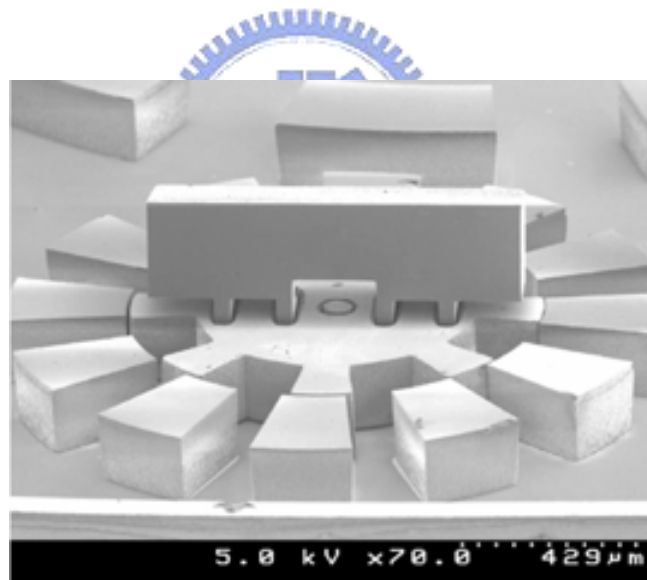


Figure 1-2. In-plane motion of micromotor. [23]

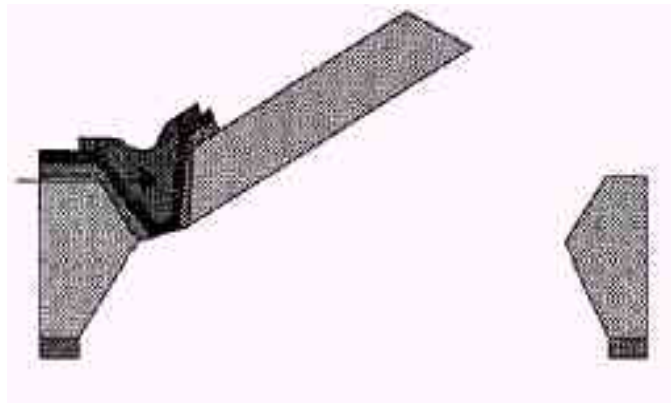


Figure 1-3. Out of plane motion of the polyimide V-groove joint. [25]

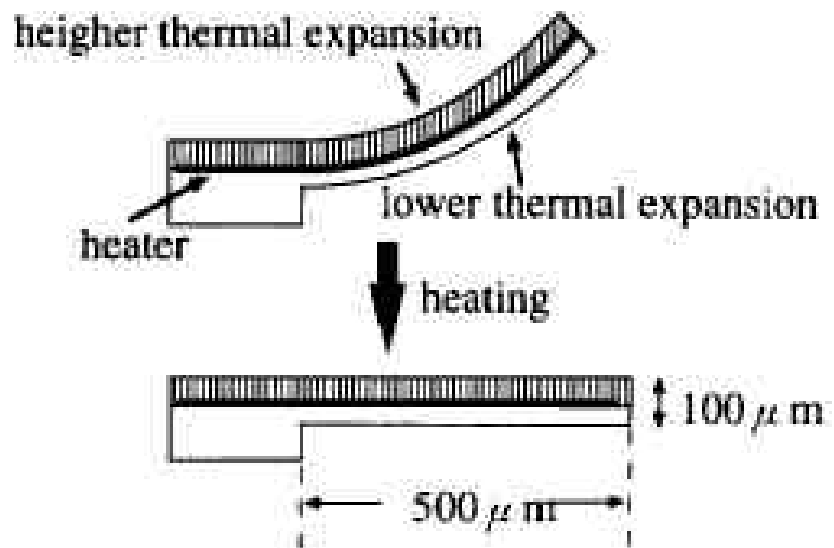


Figure 1-4. Thermally driven cantilever actuator made of polyimide. [15]

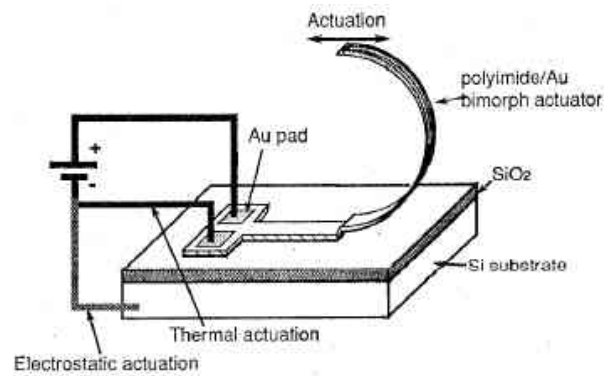


Figure 1-5. A C-shape microactuator. [26]

Micro-conveyor

The devices in MEMS are becoming more versatile and complex in recent years. Among them, micro-conveyors for locomotive mechanisms are one of the key tools to achieve automotive micro-factory or micro-warehouse systems. In general, microactuators generating large strokes and high forces are needed for micro-conveyance applications, and the actuation speed is less important [27]. Therefore, arranging microactuators in array configurations to allow the actuators working together becomes a popular approach, which not only can increase the total force and load capacity of the micro-conveyance systems, but also take advantage in MEMS batch fabrication process. Microactuators developed for micro-conveyance systems can be classified into different actuation schemes, such as thermal bimorphs [15], air jets [28-29], torsional resonators [30], electromagnetic [31-32], piezoelectric [33], and electrostatic [34]. The ciliary motion principle proposed by Ataka et al. [15] used thermal

bimorph polyimide legs which were actuated asynchronously to provide propulsion for micro-objects. This ciliary motion system based on thermal-bimorph effect shows simple fabrication process and high load capacity. However, all the reported microactuators for micro-conveyers could only move the micro objects in a single horizontal plane.

1.2. Motivation

In the dissertation, two types of the multi-dimensional motions of the microactuators are developed.

In previous literatures, most of the microactuators were designed to deflect in one dimension only. Here, an electro-thermally driven microactuator with two dimensional motions, out-of-plane and in-plane, is proposed. This microactuator comprised of a height adjuster, a moving plate, a lateral driven unit, and contact pads. The out-of-plane motion is produced due to the bimorph effect and residual stress between the layers of Au and polysilicon when they are heated. The in-plane motion is obtained by heating the lateral driven unit which consists of two adjacent beams with different cross sections but the same length, then the asymmetrical thermal expansions in two adjacent beams lead to lateral deflection.

The second kind of electrothermal microactuator may act as a basic unit for multi-level conveyers. Unlike previously reported microactuators in

micro-conveyors, the proposed device provides micro-objects conveying not only on the wafer plane but also on vertical direction. Two bimorph fingers can act as the conventional horizontal micro-conveyors unit and the height adjuster can provide an additional moving dimension in vertical direction to form a multilevel micro-conveyor basic unit. For application of micro-warehouse and micro-factory systems, the proposed height adjuster can adjust the heights of the objects to fine tune the precise positions of this micro-objects. Furthermore, the weights and sizes of micro-objects could be different and hence the objects might be moving on different vertical positions that may increase the difficulties of micro-assembly. Therefore, to assembly the three-dimensional micro-objects, multi-level conveyance provides more degree-of-freedom in control and improves the precision of assembly, by controlling the lifting heights of the height adjuster. Especially it could save more space in wafer plane because this micro-conveyor can translate the micro-objects to different height in a limited area.

1.3. Dissertation Outline

The main goal of this dissertation is to develop two kinds of microactuators with multi-dimensional motions. The detail descriptions are in the following chapters.

In Chapter 2, the concept design of these two kinds microactuators are described. And the simulation by finite element analysis is performed for the second kind microactuator.

In Chapter 3, the MUMPs fabrication process for fabricating the microactuator with two dimensional motions, especially two step releasing process is developed for this microactuator. Another microactuator is fabricated by four masks fabrication process.


In Chapter 4, the characterization and testing results are shown. Then the conclusions for these two kind microactuators are proposed in Chapter 5.

Chapter 2 DESIGN AND SIMULATION

In Chapter 1, the classification of the electro-thermal microactuators have been discussed. Here, the concept design of the electro-thermally driven microactuator with two-dimensional motions and the second kind microactuator which may act as a basic unit for multi-level conveyors are described in detail. Simultaneously, the simulations of the second kind microactuator are also performed.

2.1. Concept Design

2.1.1. An Electro-Thermally Driven Microactuator with Two-Dimensional Motions



A schematic view of the proposed microactuator is shown in Figure 2-1. This microactuator comprised of a series of $70\ \mu\text{m} \times 10\ \mu\text{m} \times 2.5\ \mu\text{m}$ bimorph beams as the height adjuster, a $500\ \mu\text{m} \times 100\ \mu\text{m} \times 2\ \mu\text{m}$ moving plate, a $600\ \mu\text{m} \times 24\ \mu\text{m} \times 2\ \mu\text{m}$ lateral driven unit with $6\ \mu\text{m}$ gap distance between two beams, and contact pads. At initial state, the height adjuster with the moving plate will bend upwards due to the residual stress difference in bimorph beams. When the height adjuster is heated, the moving plate with the lateral driven unit will bend downwards to achieve out-of-plane motion. For in-plane motion, it is obtained by heating the lateral driven unit, which consists of two beams with different cross sections. When two beams are heated by applying electric

voltage, two beams will deflect laterally due to the asymmetrical thermal expansions. Then the two-dimensional motion can be achieved by controlling the input modes of the electrical voltage.

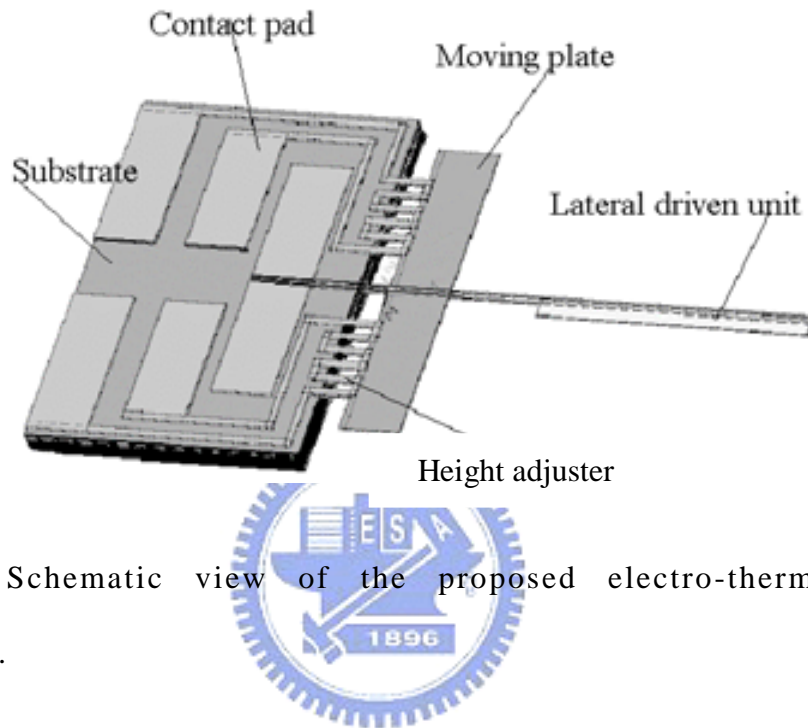


Figure 2-1. Schematic view of the proposed electro-thermally driven microactuator.

2.1.1.2. Electrothermal Microactuator for Multi-Level Conveying

The proposed microactuator is composed of two major units, as shown in Figure 2-2. One is the height adjuster, formed by two bimorph beams in the longitudinal direction with dimension of $50\ \mu\text{m}$ (L_a) \times $10\ \mu\text{m}$ (W_a) \times $4.5\ \mu\text{m}$ (h) arranged in parallel. The other is the conveying finger unit in the transversal direction, which comprises two identical bimorph finger structures with dimension about $400\ \mu\text{m}$ (L_c) \times $50\ \mu\text{m}$ (W_c) \times $4.5\ \mu\text{m}$ (h). The whole device

area including connection part of the two units is about $900 \mu\text{m} \times 100 \mu\text{m}$ where contact pads are not included. Figure 2-3 depicts operation principle of the proposed multi-level conveyance to move micro-object from plane 2 (upper plane) to plane 1 (lower plane) with lateral displacement of D and vertical displacements of Δd . Figure 2-4 shows the layout of the electrical heating resistors. There are four independent close-loops of electrical circuits acting as heating resistors with eight electrical contact pads. Two of them are for the height adjuster, which allows this microactuator to provide vertical motion. Others are for the conveying finger unit to provide the conveying motion. At initial state, the height adjuster and the conveying fingers are bent upward due to the residual stress gradient in two layers of bimorph structures. When the height adjuster unit is heated, the height of two conveying fingers is adjustable to provide conveying function in different horizontal plane by joule heating two fingers individually or simultaneously.

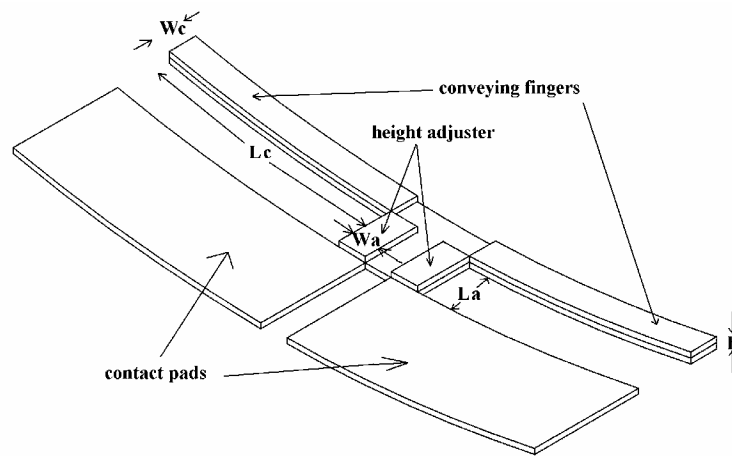


Figure 2-2. Schematic drawing of the proposed microactuator.

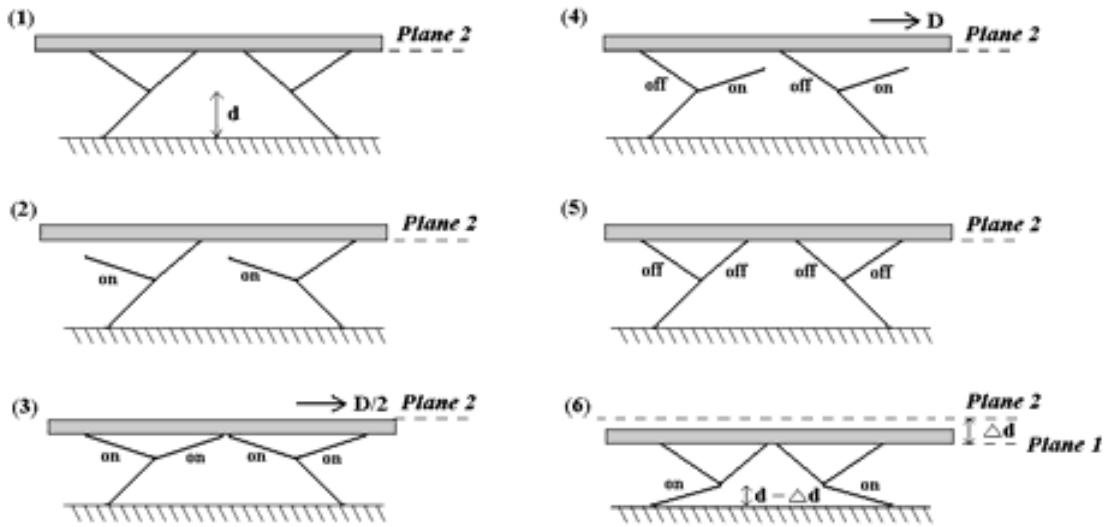


Figure 2-3. Operation principle of the proposed multi-level conveyor.

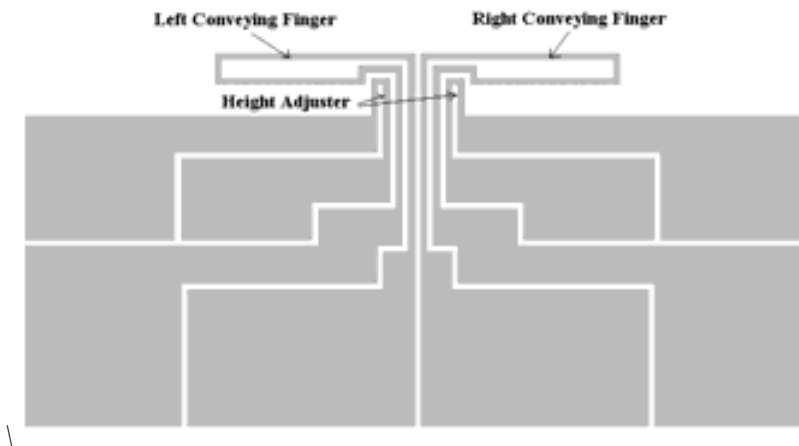


Figure 2-4. The heater circuit layout of the device.

2.2. Simulation

To perform the simulation of this microactuator, the numerical finite-element program ANSYS 5.7 is used. The microactuator is built as a 3-D model and meshed by the Solid5 element type. Solid 5 has a three

dimensional magnetic, thermal, electric, piezoelectric, and structural field capability with limited coupling between the fields. This element has eight nodes with six degrees of freedom. The bimorph structure comprises a 3 μm thick polyimide (PIX-L110SX) bottom layer, an 1.5 μm thick polyimide (PI2525) top layer, and the Cr(40Å)/Au(1000Å)/Cr(40Å) intermediate layers as the heating resistor. The physical properties of materials used in simulations are listed in Table 2. The meshed finite element model of the proposed microactuator in half-symmetry is shown in Figure 2-5.

Table 2. Material properties used in simulations.

	Polyimide PIX-L110SX	Polyimide PI2525	Au
Young's Modulus (GPa)	8.5	2.5	80
CTE (Coefficient of Thermal Expansion, 1e-6/°C)	10	40	14.3
Thermal Conductivity (W/m K)	0.167	0.167	318
Electrical Resistivity ($\Omega\text{-m}$)	1e14	1e14	23.5e-9

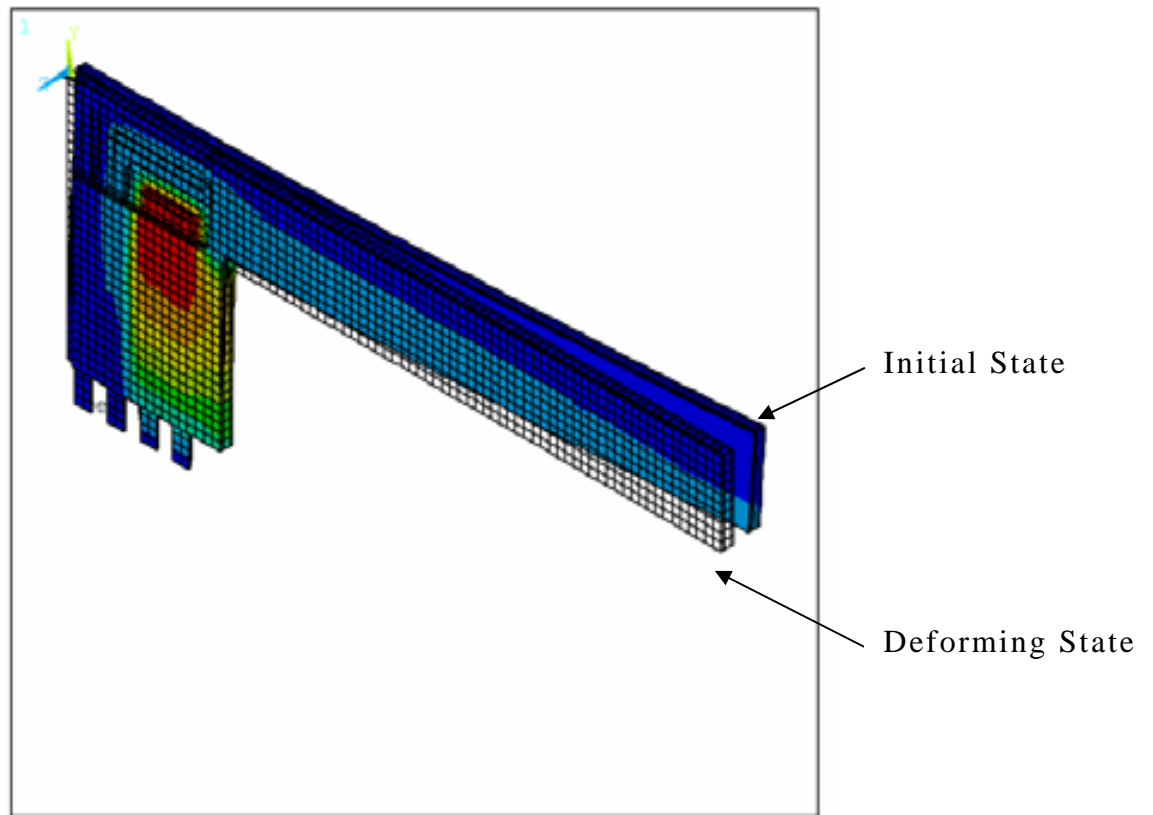


Figure 2-5. The half-symmetrical finite element 3-D model of the proposed microactuator.

The simulated finger displacements versus different input voltages are shown in Figure 2-6. It shows that the finger with 400 μm long can produce 20 μm displacements at input voltage of 2 V. The displacements of the height adjuster are also simulated as shown in Figure 2-7, where the height adjuster with 50 μm long can provide 6 μm downward displacement when the input voltage is 1 V.

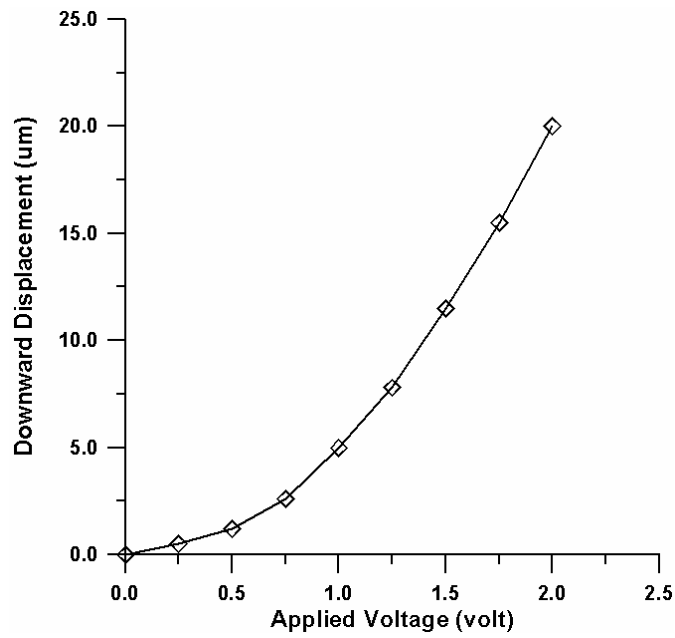


Figure 2-6. The simulated downward displacements of the finger under different input voltages.

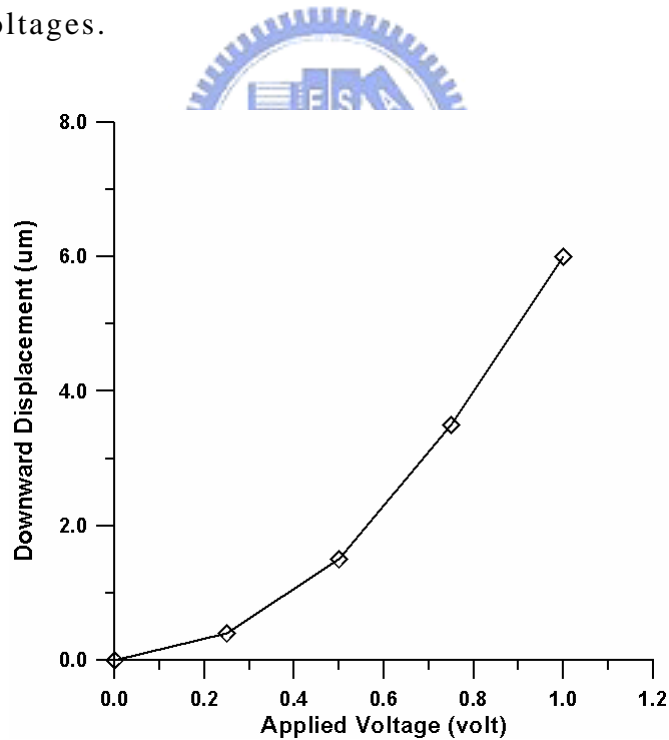


Figure 2-7. The simulated downward displacements of the height adjuster under different input voltages.

Chapter 3

FABRICATION

3.1. Fabrication of an Electro-Thermally Driven Microactuator with Two Dimensional Motions

The proposed device is fabricated by the MUMPs (Multi-User MEMS Process) process [35]. The fabrication process for this microactuator is shown in Figure 3-1. First a 600 nm low-stress LPCVD (low pressure chemical vapor deposition) silicon nitride layer is deposited on the wafers as the isolation layer (Figure 3-1(a)). A 2.0 μm phosphosilicate glass (PSG) is then deposited by LPCVD as the sacrificial layer (Figure 3-1(b)). The sacrificial layer is also lithographically patterned to form the dimples and anchor.

After etching anchor and dimples, the first structural layer of polysilicon (Poly 1) is deposited at a thickness of 2.0 μm (Figure 3-1(c)). A thin layer of PSG (200 nm) is deposited over the polysilicon as the hard mask for the subsequent polysilicon etch. The polysilicon and this PSG masking layer are patterned to form the conducting pads, moving plate, and lower layer of bimorph structures height adjuster in this first structural layer Poly 1. After etching the polysilicon, the remaining PSG hard mask is removed by RIE.

Then, another PSG layer of 0.75 μm is deposited to act as the adhesion layer to connect the moving plate and height adjuster (Figure 3-1(d)). The second structural layer, Poly 2, is then deposited with 1.5 μm and the deposition of 200 nm PSG is performed. As Poly 1 level, the thin PSG layer acts as an etch

mask. The Poly 2 and this PSG layer are then patterned to form the lateral driven unit (Figure 3-1(e)). After that, the masking PSG layer is removed.

The final deposited layer is the 0.5 μm metal layer, as shown in Figure 3-1(f). The metal on the beam structures that are produced in POLY 1 level form the bimorph beams.

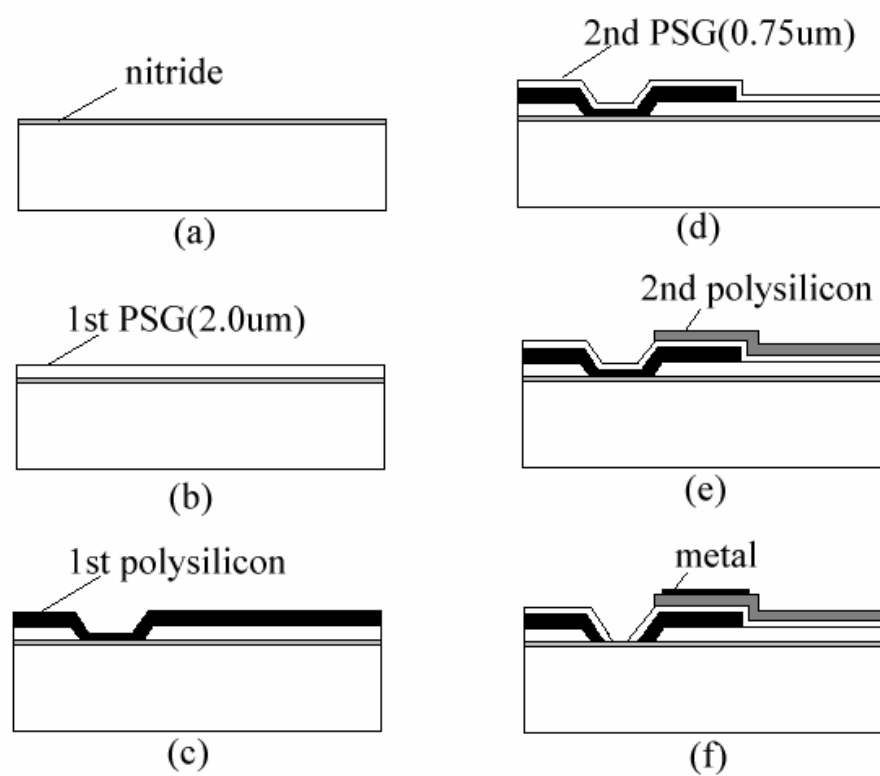


Figure 3-1. Fabrication process.

The releasing process, in the beginning, was performed by immersing the chip in a bath of 49% HF(at room temperature) for about 10 minutes, several

minutes in DI water and alcohol to reduce stiction, then at least 10 minutes in an oven at 110 °C. The fabricated result from this one-step releasing is shown in Figure 3-2. It is found that the moving plate and height adjuster are separated. The reason is that this device has several PSG layers. The upper 0.75 μm PSG layer between the moving plate and height adjuster (10 μm width) is used as an adhesion layer to connect the moving plate and height adjuster, and the lower 2 μm PSG layer under the moving plate is used as the sacrificial layer. The etching time to remove the sacrificial layer is about 10 minutes in HF solution, but this etching time will cause the adhesion PSG layer to be depleted thoroughly also, then the moving plate and height adjuster can no longer be connected. To solve this problem, we shorten the releasing time by immersing the chip in a bath of 49 % HF (at room temperature) for 8 minutes, following process is the same as above. But we find the moving plate and the substrate are sticted together (Figure 3-3).

In order to avoid the adhesion PSG layer being etched away completely or the moving plate be sticted, a two-step releasing process is proposed. The upper 0.75 μm PSG layer is etched first, and another mask is added to protect the PSG between the moving plate and bimorph beams. After that, the chip is immersed into B.O.E (Buffer Oxide Etchant) for 2 hours to release the PSG sacrificial layer, then several minutes in DI water and 30 minutes in alcohol, which is the same as the one-step releasing processes. After modification on the release process, the moving plate connected with the height adjuster is successfully fabricated, as shown in Figure 3-4, the SEM of the height adjuster

with moving plate as shown in Figure 3-5. The top view of the fabricated result is shown in Figure 3-6. The SEM of the lateral driven unit and height adjuster with moving plate are shown in Figure 3-7 and Figure 3-8, respectively.

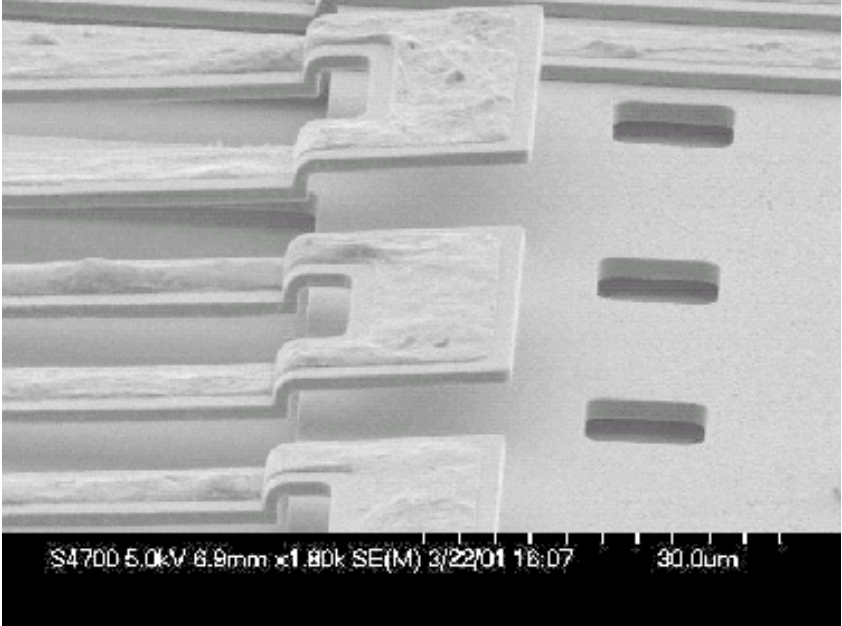


Figure 3-2. The initial fabrication result by one-step releasing process.

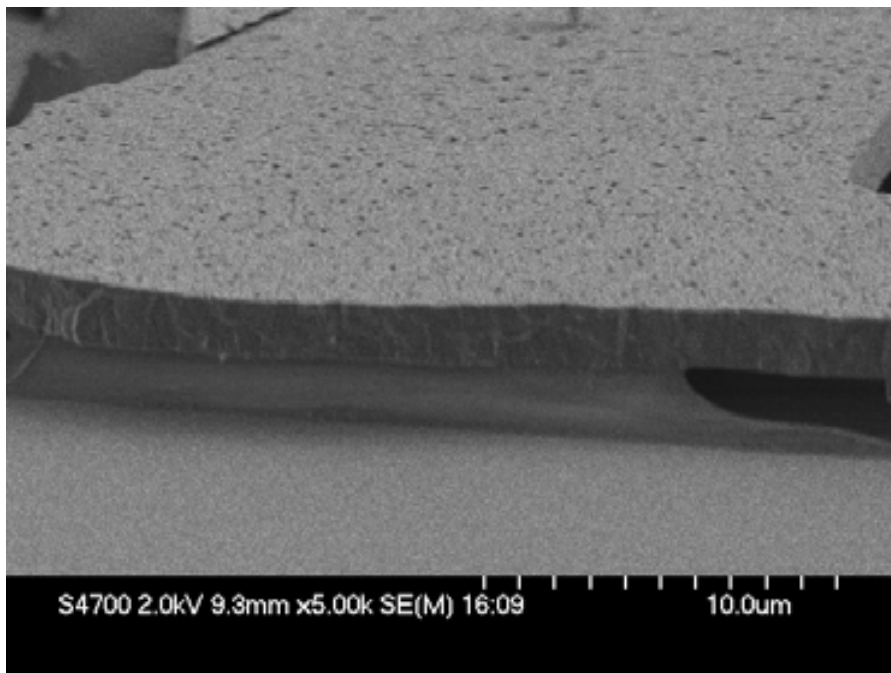


Figure 3-3. The moving plate and the substrate are stuck together.

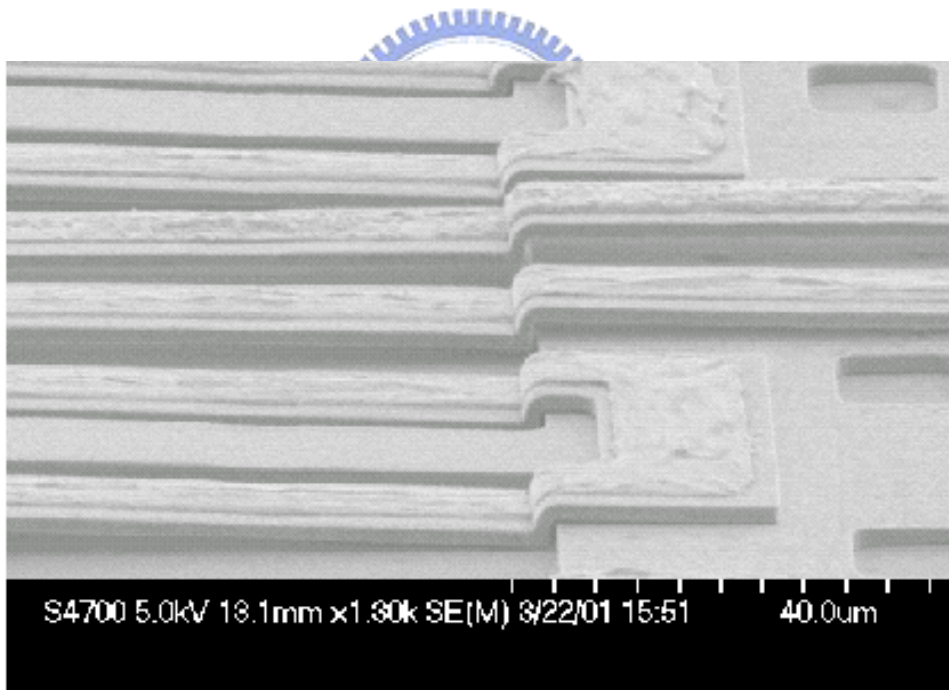


Figure 3-4. The final fabrication result by modified two-step releasing process.

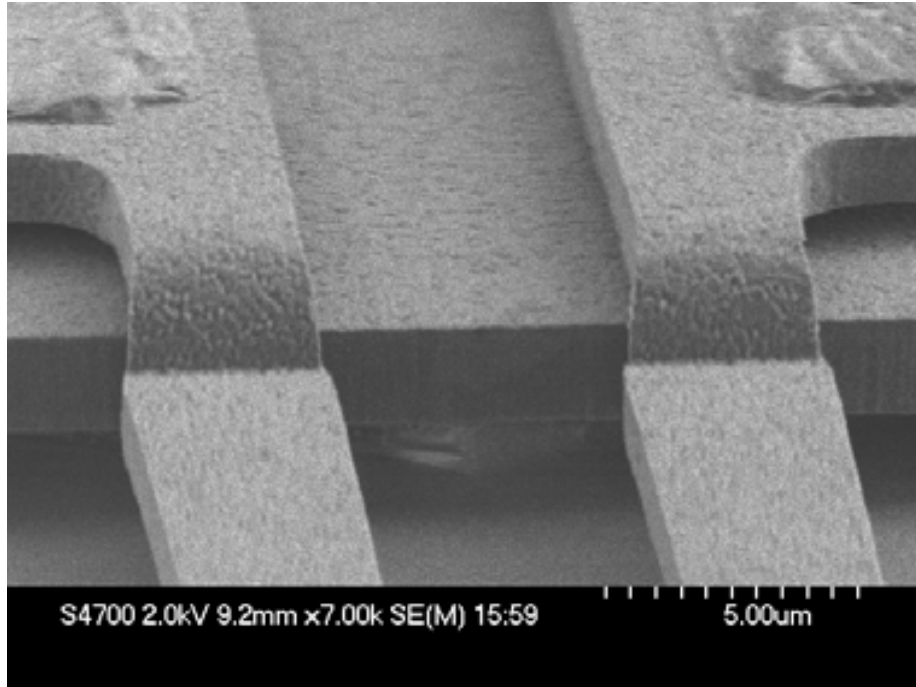


Figure 3-5. The SEM of the height adjuster with moving plate.

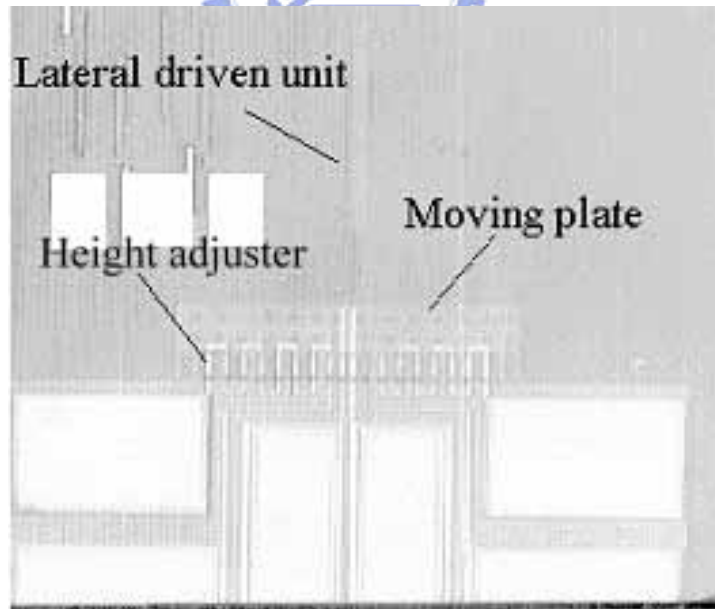


Figure 3-6. The top view of the fabricated result of the microactuator.

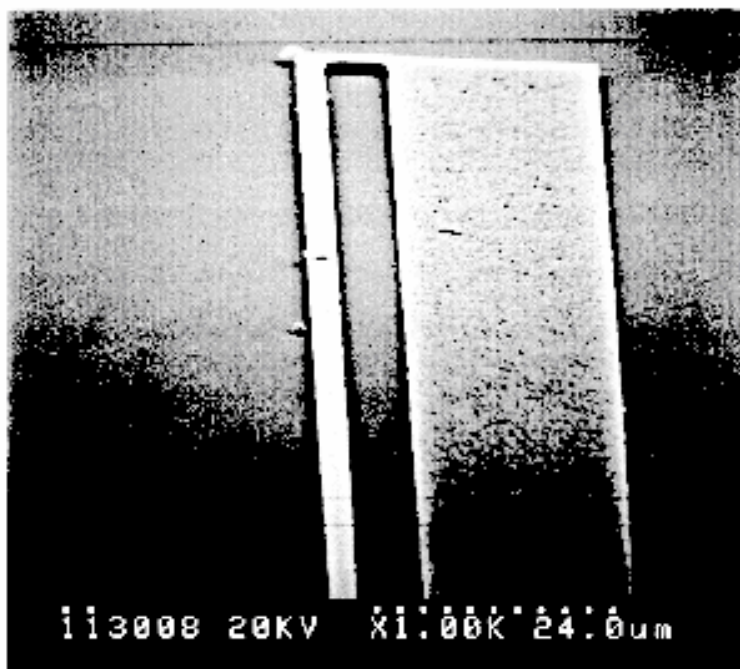


Figure 3-7. The SEM of the lateral driven unit.

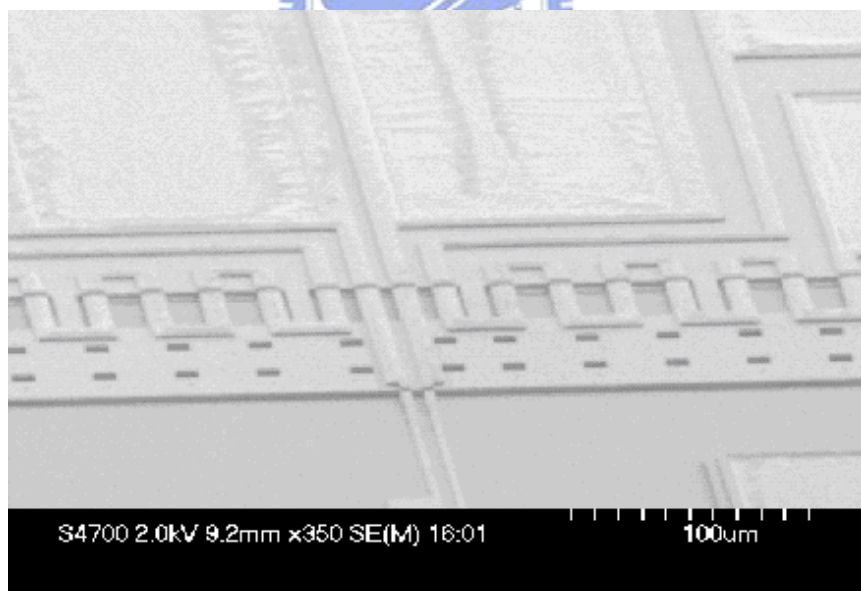


Figure 3-8. The SEM of the height adjuster, moving plate and contacted pads.

3.2. Fabrication of an Electro-Thermally Microactuator for Multi-Level Conveying

The microactuator proposed here is batch-fabricated by surface-micromachining technique. The four-mask fabrication process is outlined in Figure 3-9. First, the 1 μm thick aluminum sacrificial layer is deposited by thermal evaporation. Then it is patterned to form the anchor by mask 1 (Figure 3-9(a)). Polyimide (PIX-L110SX) of 3 μm thickness with lower thermal expansion coefficient is spun coated and cured as the bottom layer of the bimorph structure. Metallic microheater (Cr(40Å)/Au(1000Å)/Cr(40Å)) is formed by lift-off process with mask 2, as shown in Figure 3-9(b). The Cr layer is used to enhance the adhesion between the Au and polyimide. After that, a 1000Å thick Ni is deposited and patterned by mask 3 to protect the microheater of the height adjuster in the following RIE (Reactive Ion Etching) process (Figure 3-9(c)). On top of them, the 1.5 μm thick polyimide (PI2525) as the top layer with higher thermal expansion coefficient is coated and cured. Following, a 1000Å thick nickel is evaporated and patterned by mask 4 as hard mask, as shown in Figure 3-9(d). The top and bottom polyimide layers are then patterned by RIE using oxygen gas.

The releasing process is performed by immersing the wafer in aluminum etchant for 10 minutes, rinsing in DI (Deionized) water for 5 minutes and in IPA (Isopropyl Alcohol) for 30 minutes to reduce stiction problem sequentially. Then, the device is placed on hotplate at 110 for

5 minutes to suspend the microactuator, as shown in Figure 3-9(e).

The perspective view and close-up view of the fabricated microactuators are shown in Figure 3-10 and Figure 3-11, respectively.

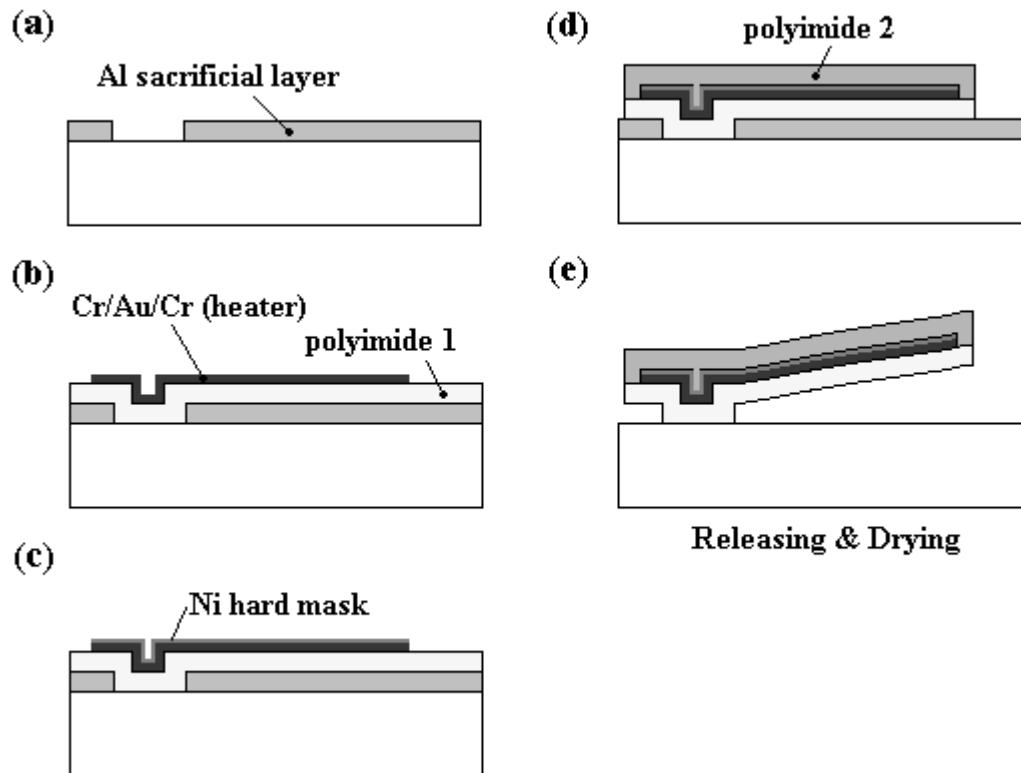


Figure 3-9. Fabrication process.

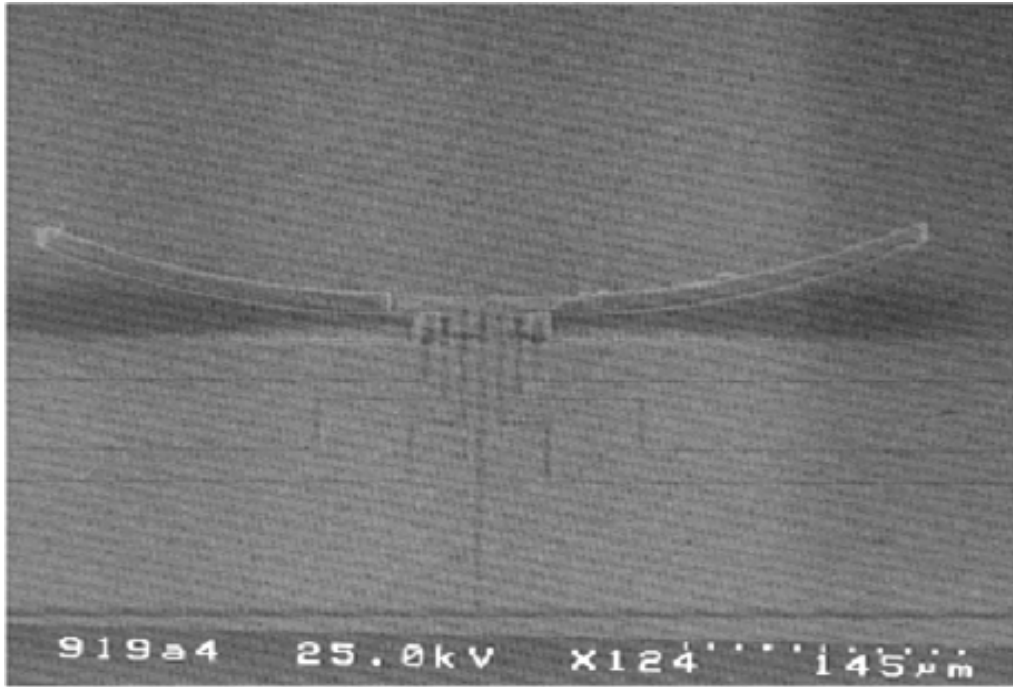


Figure 3-10. Scanning electron microscopes of the fabrication results.

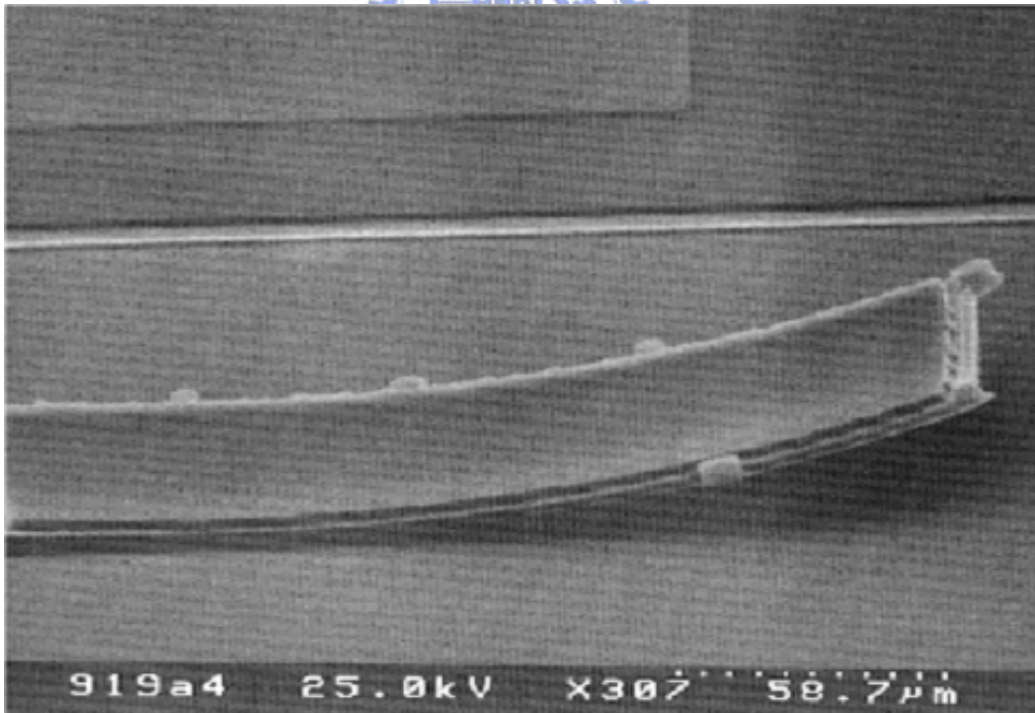


Figure 3-11. Close-up view of the finger.

Chapter 4

CHARACTERIZATION AND RESULTS

In Chapter 3, the fabrication process for both the microactuator with two dimensional motions and the microactuator for multi-level conveying are described. Here, the details of the characterization and the testing results of them are proposed below.

4.1. Characterization of an Electro-Thermally Driven Microactuator with Two Dimensional Motions

Whole measuring system including microscope, station, the CCD camera, computer with image capture and power supplier is shown in the Figure 4-1.

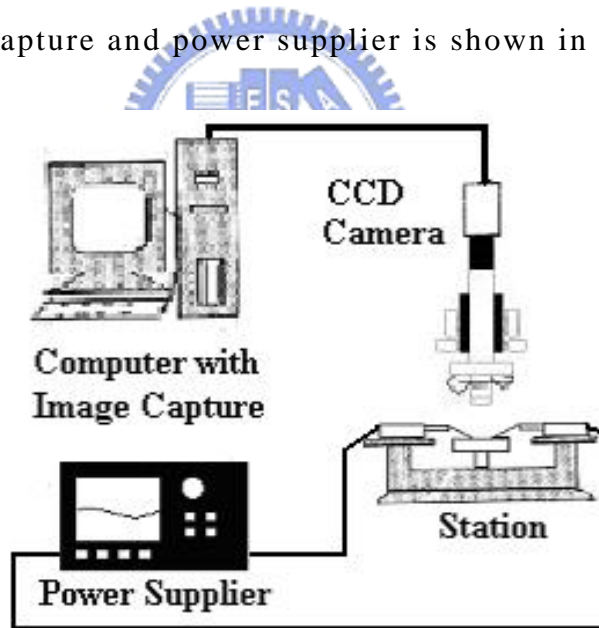


Figure 4-1. Schematic drawing of the measurement system.

In testing, various dc voltages are applied to the contact pads to generate

different motion modes. The lateral displacements are measured from the pictures captured by image capture software from the video. The downward displacements are determined by focus/defocus method on the optical microscope, which gives the measurement error about 1 μm .

In the initial state, it is observed that the end of the moving plate curled up about 12 μm from the substrate, 4 degrees in angular displacement, due to the residual stress in bimorph beams. Figure 4-2 shows the testing results of the lateral driven unit under various input voltages. The lateral displacement up to 14 μm can be achieved at input voltage of 7 V. Also, the testing results of the height adjuster are shown in Figure 4-3, where 12 μm downward displacement is achieved at 5 V before touching the substrate.

In addition, two-dimensional tests are performed to see if there is coupling effect where both height adjuster and the lateral driven unit are operated under the same input voltages. Figure 4-4 shows that no matter the lateral driven unit is operated or not, the vertical displacements of height adjuster under different voltages are not affected. Similar testing results are also found in lateral displacements. No matter the height adjuster is turned on or turned off, the maximum difference in lateral displacement is only about 1 μm , which is within the measurement error range. From Figure 4-4, it is shown that the coupling effect between the vertical and lateral direction is very small, and these testing results demonstrated the capability of providing two dimensional motions with the proposed microactuator.

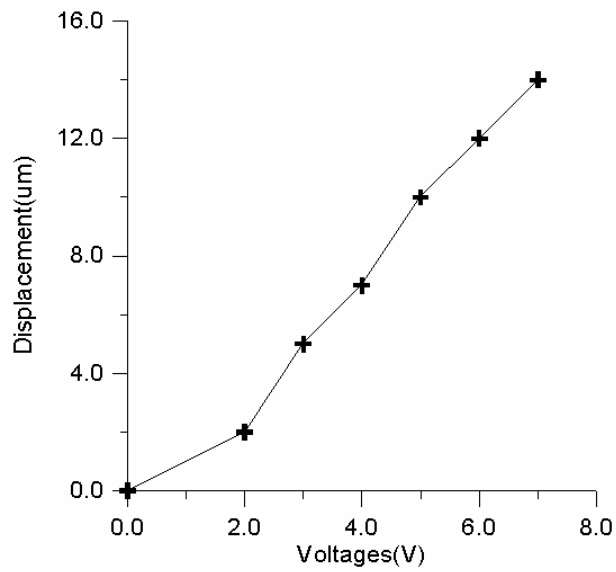


Figure 4-2. The measured lateral displacements of the lateral driven unit under different input voltages.

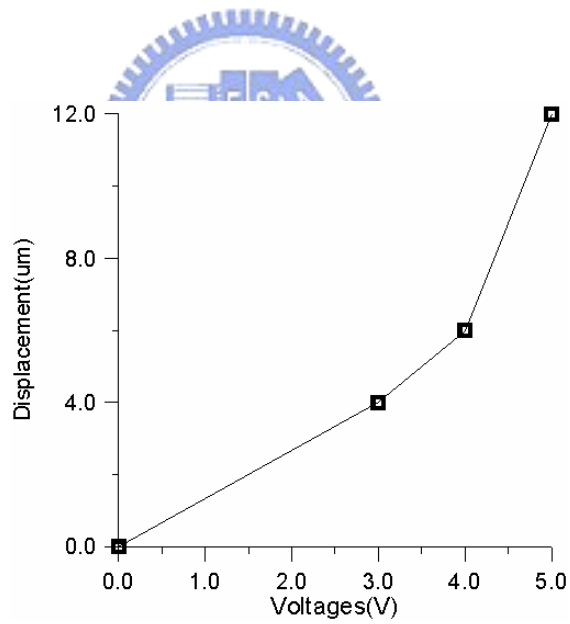


Figure 4-3. The measured downward displacements at the end of the moving plate under different input voltages.

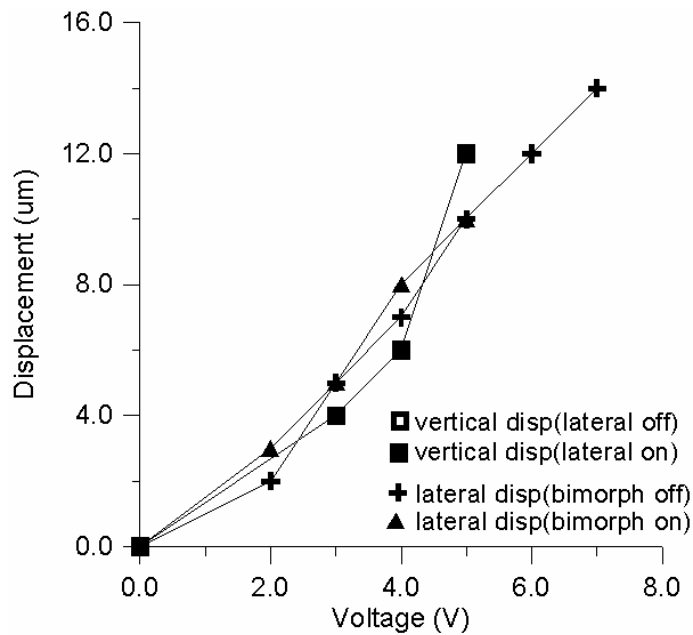


Figure 4-4. The measured displacements in coupling test where the lateral driven unit and bimorph beams are operated at the same input voltages simultaneously.



4.2. Characterization of an Electro-Thermally Microactuator for Multi-Level Conveying

It is observed that the ends of the conveying finger and the height adjuster curled up about 18 μm and 5 μm from the substrate, respectively, due to the residual stresses in bimorph beams. In testing, various dc voltages are applied to the contact pads to generate different actuation modes.

Figure 4-5 shows comparison of the simulation and testing results of the finger-tip displacements under various input voltages. In testing, the downward displacement up to 18 μm are achieved at input voltage of 2 V. The maximum deviation between simulation and testing results is within 10%. In

addition, the simulation and testing results of the height adjuster are shown in Figure 4-6. In testing, 5 μm downward displacement is achieved at 1 V before touching the substrate, and the deviation between the simulation and measurement results is within 20%. The approximate maximum load per microactuator is about 0.196 mg., which is estimated by calculating the elastic-mechanical stiffness of the adjuster/fingers structures. According to experimental results, the lateral displacement of the conveying finger at output vertical displacement of 13-15 μm is about 0.2-0.3 μm . Hence, the estimated maximum velocity for conveyance is about 1.0-1.5 $\mu\text{m}/\text{sec}$ at maximum operating frequency of 5 Hz.

Further, thermal coupling effect of the height adjuster and the conveying fingers are examined by multi-dimensional motion testing. First, the height adjuster is actuated at 1 V, and then different voltages are applied to the conveying fingers to observe whether the conveying finger is affected by the height adjuster. The height adjuster deflects 5 μm in downward direction at one volt while the conveyor fingers are not actuated. Figure 4-7 shows the measured displacements of the height adjuster at 1 V while applying different voltages to the conveying fingers simultaneously. As shown in Figure 4-7, the deviations on positions of height-adjuster end are negligible and that are all within measurement resolution of 1 μm . It is also found that the tips of conveying fingers deflect 18 μm at 2 volts while the height adjuster still delivers 5 μm downward displacement at 1 volt. Testing results indicate that the displacements of height adjuster are not affected by operating conveying

fingers. Similar testing processes are also performed to the conveying fingers. Figure 4-8 shows the load-position curves of the conveying finger tip with simultaneous actuation of height adjuster. Different curves in Figure 4-8 represent different dc driving voltages of the height adjuster. From this testing, it is observed that the downward deflection of the conveying finger tip relative to the end of the height adjuster is affected by the actuation of height adjuster slightly. For instance, the downward displacements of conveying finger actuated at 1.5 volts with height adjuster actuated at 0.75 volts and 0 volt are 14.5 μm and 10.5 μm respectively. However, the height adjuster produces about 3 μm downward displacement at 0.75 volts. Hence, the absolute downward displacement of conveying finger affected by thermal crosstalk from height adjuster is actually around 1 μm . In testing, the increased downward displacements of conveying finger are all below 10% of the displacements without actuating the height adjuster.



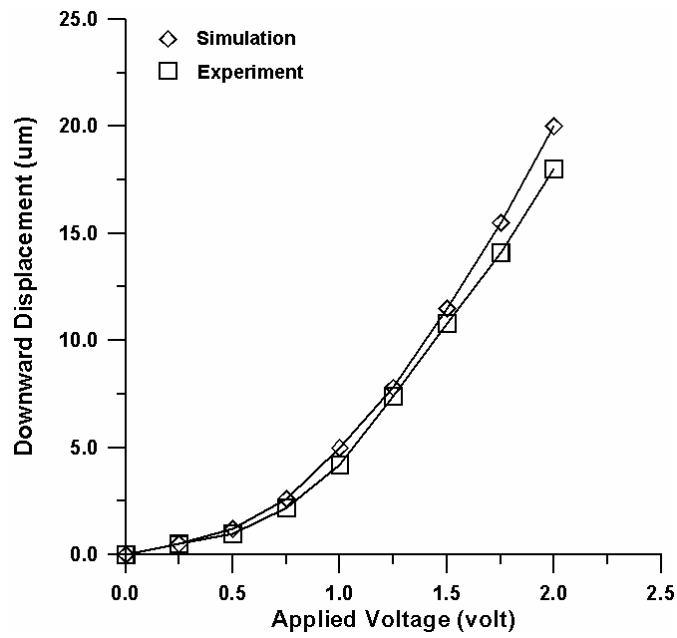


Figure 4-5. The simulated and calibrated downward displacements of the conveying finger under different input dc voltages.

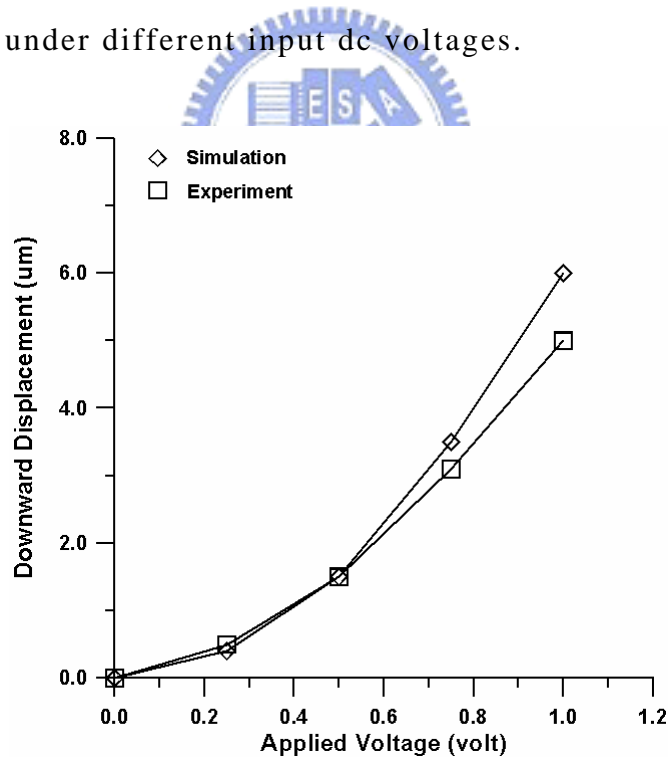


Figure 4-6. The simulated and calibrated downward displacement of the height adjuster under different input dc voltages.

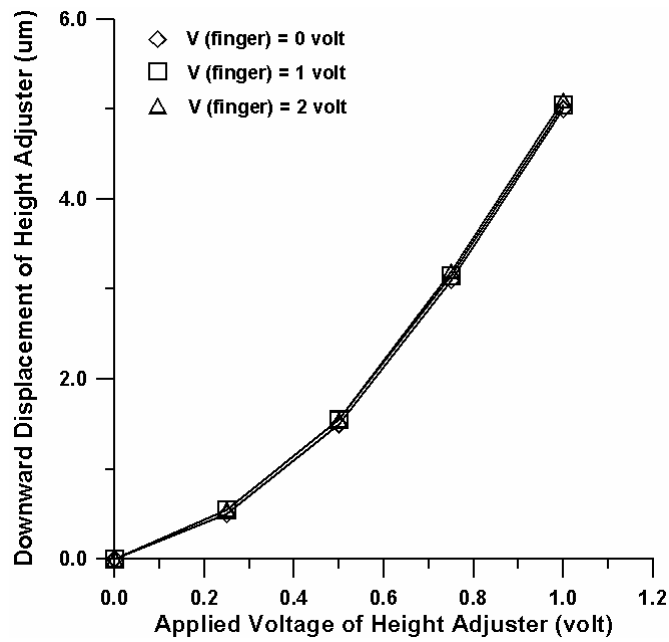


Figure 4-7. The measured displacements at the end of height adjuster in coupling test, where the height adjuster is actuated firstly, and then different input voltages are applied to the conveying fingers.

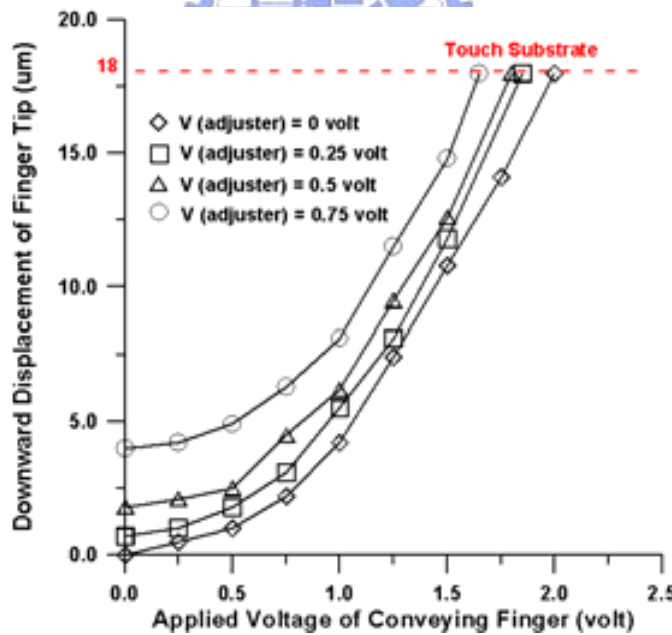


Figure 4-8. The measured displacements of finger tip in coupling test, where the finger is actuated first, and then different input voltages are applied on the height adjuster.

Chapter 5

CONCLUSIONS

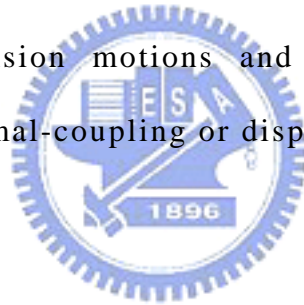
5.1. Summary

Two kinds of electro-thermally driven microactuators with multi-dimensional motions are designed, fabricated, and tested. Some features of electro-thermally driven microactuator with two dimensional motions are summarized below: () This microactuator is shown to be able to deflect in two dimensions and nearly uncoupled. () This microactuator is self assembled and does not need any locking structures or external manipulation. () Modified releasing processes is helpful in fabricating this microactuator.

As about the microactuator for multi-level conveyance, beside the conventional horizontal conveying, a height adjuster is included to enhance the conveying range from single-plane to multi-level conveying. It is also shown that the proposed device can be operated at input voltage below 3 volts. The simulation results agree with the test results. From thermal coupling tests, this device is shown to have little cross talking while heating the height adjuster and two conveying fingers. It means that the height adjuster and two fingers can be operated almost independently. The material selections and dimension designs of this microactuator can be further investigated to improve the performance.

5.2. Discussions

The multi-dimensional motions microactuators proposed here are all basically consisted of two actuation parts. The deflecting directions of each actuation part of the same microactuator are different so as to exhibit spatial motions. However, actuation principles are all based on electro-thermal joule heating, therefore, thermal-coupling problems may be encountered and should be minimized as possible in design. In current research, the use of low thermal conductivity materials such as polyimide or polymers and configurations with reduced thermal-flow cross section areas results in larger thermal resistance between actuation parts. From the experimental results, the proposed microactuator of two-dimension motions and microactuator for multi-level conveying showed little thermal-coupling or displacement-coupling problems.



REFERENCES

1. S. Fatikow and U. Rembold, "Microsystem Technology and Microrobotics", Springer, ch. 3, 1997.
2. W. S. N. Trimmer, "Microrobots and Micromechanical System", Sensors and Actuators A, vol. 19, pp.267-287, 1989.
3. Gad el Hak Mohamed, "The MEMS Handbook", CRC press, ch. 2, 2001.
4. C. C. Lee and W. Hsu, "Method on Surface Roughness Modification to Alleviate Stiction of Microstructures", J. Vacuum Science and Technologies B, vol. 21, no. 4, pp.1505-1510, 2003.
5. K. E. Petersen, "Silicon as a Mechanical Material", Proc. IEEE, vol.70, no.5, p.420-457, 1982.
6. K. D. Wise, T. N. Jackson, N. A. Masnari, and M. G. Robinson, "Fabrication of Hemispherical Structures Using Semiconductor Technology for Use in Thermonuclear Fusion Research", American Vacuum Society, pp. 936-939, 1979.
7. C. H. Lin, Y. C. Lo, and W. Hsu, "Micro-Fabrication of Hemispherical Poly-Silicon Shells Standing on Hemispherical Cavities", SPIE's New Millennium'03, Gran Canaria (Canary Islands), Spain, 2003.
8. L. S. Fan, Y. C. Tai, and R. S. Muller, "IC-processes Electrostatic Micromotors," Sensors and Actuators A, vol.20, pp. 41-48, 1989.
9. M. Mehregany, P. Nagarkar, S. D. Senturia, and J. H. Lang, "Operation of Microfabricated Harmonic and Ordinary Side-Drive Motors," Proc. 3rd. IEEE MEMS Workshop, Napa Valley, CA, pp. 1-8, 1990.
10. W. C. Tang, T. U. Chong, H. Nguyen, and R. T. Howe, "Laterally Driven Polysilicon Resonant Microstructures," Sensors and Actuators A, vol.20, pp. 25-32, 1989.
11. T. Akiyama, and K. Shono, "Controlled Stepwise Motion in Polysilicon Microstructures," J. Microelectromechanical Systems, vol.2, no.3, pp. 106-110,

1993.

12. A. J. L. Yeh, H. Jiang, and N. C. Tien, "Integrated Polysilicon and DRIE Bulk Silicon Micromachining for an Electrostatic Torsional Actuator," *J. Microelectromechanical Systems*, vol.8, no.4, pp. 456-465, 1999.
13. A. M. Flynn, L. S. Tavrow, S. F. Bart, R. A. Brooks, D. J. Ehrlich, K. R. Udayakumar, and L. E. Cross, "Piezoelectric Micromotors for Microrobots," *J. Microelectromechanical Systems*, vol. 1, pp. 44-51, 1992.
14. I. J. B. Vishniac, "The Case for Magnetically Driven Microactuators," *Sensors and Actuators A*, vol.33, pp. 207-220, 1992.
15. M. Ataka, A. Omodaka, N. Takeshima, and H. Fujita, "Fabrication and Operation of Polyimide Bimorph Actuators for a Ciliary Motion System", *J. Microelectromechanical Systems*, vol.2, no.4, pp. 146-150, Dec. 1993.
16. S. P. Timoshenko, "Analysis of Bi-Metal Thermostats", *J. Opt. Soc. Am.*, vol. 11, pp. 233-255, 1925.
17. W. Riethmuller, and W. Benecke, "Thermally Excited Silicon Microactuators" *Electron Devices, IEEE Transactions on*, vol. 35, pp. 758-763, June 1988.
18. H. Guckel, J. Klein, T. Christenson, K. Skrobis, M. Landon, and E. G. Lovell, "Thermo-magnetic metal flexure actuators", *Tech. Digest, IEEE Solid State Sensor and Actuator Workshop*, pp. 73-75, 1992.
19. C.H. Pan, and W. Hsu, "An electro-thermally driven polysilicon microactuator", *J. Micromech. Microeng.*, vol. 7, pp. 7-13, 1997.
20. M. Kohl and K. D. Skrobanek, "Linear microactuators based on shape memory effect", *Sensors and Actuators A*, vol. 70, pp. 104-11, 1998.
21. S. Ashley, "Getting a microgrip in the operating room", *Mechanical Engineering*, pp. 91-93, 1996.
22. W. C. Tang, T. C. H. Nguyen, and R. T. Howe, "Laterally Driven Polysilicon Resonant Microstructures". *Proc. of IEEE Micro Electro Mechanical Systems*: 53-59, 1989.

23. A. A. Yasseen, J. Mitchell, T. Streit, D. A. Smith, and M. A. Merhergany, "Rotary Electrostatic Micromotor 1x8 Optical Switch", Proc. of Micro Electro Mechanical Systems, MEMS 98, The 11th Annual International Workshop on. pp 116-120, 1998.
24. J. R. Reid, V. M. Bright, and J. T. Butler, "Automated Assembly of Flip-up Micromirrors", Sensors and Actuators. A66: 292-298, 1998.
25. T. Ebefors, E. Kälvesten, and G. Stemme, "Dynamic Actuation of Polyimide V-Groove Joints by Electrical Heating", Sensors and Actuators. A67: 199-204, 1998.
26. G. Lin, C. J. Kim, S. Konishi, and H. Fujita, "Design, Fabrication and Testing of a C-shape Actuator", Tech. Digest, 8th International Conference. Solid-State Sensors and Actuators(Transducers '95/ Eurosensors) Stockholm, Sweden. pp. 416 –419, 1995.
27. R. S. Fearing, "Powering 3-Dimensional Microrobots: Power Density Limitations", IEEE Int. Conf. on Robotics and Automation, Tutorial on Micro Melectronics and Micro Robotics, 1998.
28. S. Konishi and H. Fujita, "A Conveyance System Using Air Flow Based on the Concept of Distributed Micro Motion Systems", Journal of Microelectromechanical Systems, Volume: 3, No, 2, pp. 54-58, 1994.
29. K. S. J. Pister, R. S. Fearing, and R.T. Howe, "A Planar Air Levitated Electrostatic Actuator System", Proc. IEEE 5th Workshop on Micro Electro Mechanical Systems, Napa Valley, CA, pp. 67-71, 1990.
30. Y. Mita, S. Konishi, and H. Fujita "Two Dimensional Micro Conveyance Systems with Through Holes for Electrical and Fluidic Interconnection", Int. Conf. Solid State Sensors and Actuators (Transducers '97), Chicago, Volume: 1, pp. 16-19, 1997.
31. C. Liu, T. Tsai, Y. C.Tai, W. Liu, P. Will, and C.M. Ho, "A Micromachined Permalloy Magnetic Actuator Array for Mmicro Robotics Assembly Systems",

- Int. Conf. Solid-State Sensors and Actuators (Transducers '95), Volume: 1, pp. 328-331, 1995.
32. H. Nakazawa, Y. Watanabe, O. Morita, M. Edo, and E. Yonezawa, “The Two-Dimensional Micro Conveyor: Principles and Fabrication Process of the Actuator”, Int. Conf. Solid State Sensors and Actuators (Transducers '97), Chicago, Volume: 1, pp. 33 –36, 1997.
33. T. Furuhashi, T. Hirano, and H. Fujita “Array-Driven Ultrasonic Microactuators”, Int. Conf. Solid-State Sensors and Actuators (Transducers '91), pp.1056 –1059, 1991.
34. M. Edo, Y. Watanabe, O. Morita, H. Nakazawa, and E. Yonezawa, “Two-Dimensional Micro Conveyor with Integrated Electrostatic Actuators”, 12th IEEE International Conference on Micro Electro Mechanical Systems (MEMS '99), pp. 43-48, 1999.
35. D. Koester, R. Majedevan, A. Shishkoff, K. Marcus, “Multi-User MEMS Processes (MUMPS) Introduction and Design Rules, rev.4”, MCNC MEMS Technology Applications Center, Research Triangle Park, NC 27709, USA, July 1996.

